

Design and realization of a novel planar array antenna and low power LNA for Ku-band small satellite communications

Lida KOUHALVANDI*, Osman CEYLAN, Selçuk PAKER, Hasan Bülent YAĞCI

Department of Electronics and Communication Engineering, İstanbul Technical University, İstanbul, Turkey

Received: 21.09.2015

Accepted/Published Online: 11.05.2016

Final Version: 10.04.2017

Abstract: This article presents both a four-element novel microstrip array antenna and a low noise amplifier (LNA) for a Ku-band small satellite receiver. It includes all design details with measurement results of the fabricated array antenna and LNA. Measured minimum and maximum gains of the proposed antenna are 10.1 and 10.9 dBi in 11.9–12.9 GHz band frequency. The designed LNA has a noise figure lower than 1.5 dB and gain higher than 8 dB (at 2 V, 10 mA biasing). In order to reduce the design period and cost, discrete components are chosen and a hetero-junction FET is used as the active component because of better Ku band performance and stability. The simulation and fabricated measurement outcomes of the array antenna and LNA show competent and qualified matching that can be practically used together.

Key words: Ku-band, planar array antenna, low noise amplifier, small satellite communications

1. Introduction

Satellite technologies have been changing rapidly. Especially small satellites (<100 kg) deployed at low earth orbit (LEO) are preferred for many applications due to their low operating and manufacturing costs. Nowadays, small satellites produce more data such as high resolution images and high accuracy sensor information because of technical developments in small satellite subsystems. Therefore, wider bandwidth and higher carrier frequency are required to transmit large amounts of data from the small satellite in a short time. These days the X and Ku bands are in use for small satellite communication due to their advantages of wide bandwidth [1].

Patch array antennas are extensively used in many antenna systems because of their reasonable bandwidth, polarization purity, low cost, simplicity, easy fabrication, and power-handling capability [2]. Planar array antennas have additional significant advantages for small satellites. First of all, they do not need a deployment system. Therefore, additional protection units and mechanical tools for deployment are not needed. This results in less weight and smaller size for the small satellite. Size of the antenna is also small at the X and Ku bands. It provides additional space for extra solar panels.

As a rule of thumb, the first stage of a receiver has the upmost effect on the total noise figure (NF) of the receiver. Therefore, low noise amplifiers are preferred at the input stages after the receiver antenna. Gain, NF, linearity, and power consumption are the major specifications in designing LNAs [3]. Designing an LNA at the Ku band brings some significant problems such as low frequency stability, high component losses, and limited discrete devices for the Ku band in the market.

*Correspondence: lida.kouhalvandi@yahoo.com

The motivation of this paper is the design and implementation of a low cost planar array antenna and LNA with discrete components for a Ku-band small satellite receiver. Although there are many reported wideband MMIC or RFIC LNAs, most of them are not packaged and not considered under space conditions. In particular, research (university) satellites may need several updates during the design period due to other subsystem requirements. Discrete designs provide short redesign time and tuning possibility.

According to link budget calculation for 650 km altitude, at least 9.5 dB gain is required at the desired band around 12.5 GHz with 10 dB link margin (free space path loss = -170 dB, satellite receiver sensitivity = -85 dBm, ground station transmitter antenna gain = 36 dBi, ground station transmitter output power = ~50 W). All passive components and soldering material of the array antenna and LNA are suitable for harsh space conditions such as vibration, high temperature change, and vacuum.

In this paper, design details and simulation and measurement results of a planar novel shaped array antenna and LNA are presented. The combiner structure of the antennas is located under the ground metal of the array antenna so that it prevents interference between antennas and the combiner circuit and the designed LNA includes a commercially available HJ-FET with high temperature stability. The presented article consists of three sections after the introduction. In parts two and three simulation and manufactured measurement results of the array antenna and LNA are explained and represented precisely. In part four, brief and accurate descriptions of the proposed array antenna with LNA as the concluding part of this work are given in meticulous terms.

2. Microstrip array antenna

According to the link budget of this study, at least 9.5 dB gain is required for the microstrip array antenna in order to obtain 10 dB link margin. At least 10 dB gain is aimed for the final antenna at the desired bandwidth.

The planar antenna's performance is directly related to its substrate. Therefore, low loss Taconic TSM-30 substrate ($\epsilon_r = 3$ and loss tangent = 0.0013) is chosen and its high thermal stability makes it more suitable for small satellite applications. Array antenna topology is used for increasing directivity and gain.

The proposed antenna consists of two structures: array antenna and combiner. At the top of the antenna, there are 4 small patch antennas and at the bottom a combiner for the patch antennas is located. The patch antennas, combiner, and whole structure are designed and simulated on Ansoft HFSS software. Figure 1 shows the cross section of the antenna structure; the upper and bottom substrates' thicknesses are 1.52 mm and 0.76 mm, respectively.

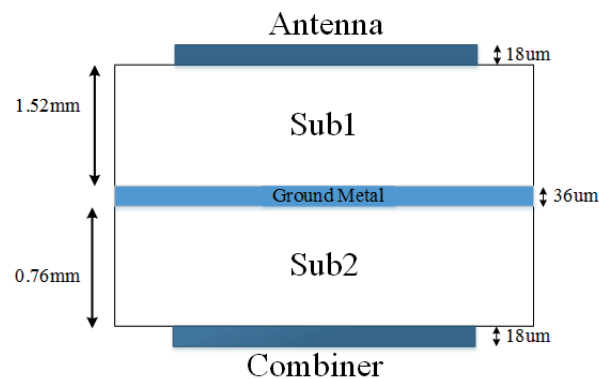


Figure 1. Antenna cross-section view.

A basic formulation [4] was considered for the initial values of antenna length (W_y) and width (W_x) for the Ku band. Prasad and Chattoraj's study [5] was modified to obtain the required technical specifications such as gain and directivity. Through Figure 2 improved designs of the proposed single antenna are presented. The antenna design is started by simulating Ant 1 [5] and then improved by removing a part of the patch (Ant 2). Ant 3, which is used in this work, can be achieved by not only using optimization for all parameters mentioned in Table 1, but also by applying a rectangular patch antenna over Taconic TSM-30 substrate $\epsilon_r = 3$, with the height of 1.52 mm. It can be noted that optimization is performed in order to obtain a small single antenna with high gain and wide bandwidth. Figure 3 demonstrates bandwidth enhancement under -10 dB from 360 MHz to 1530 MHz.

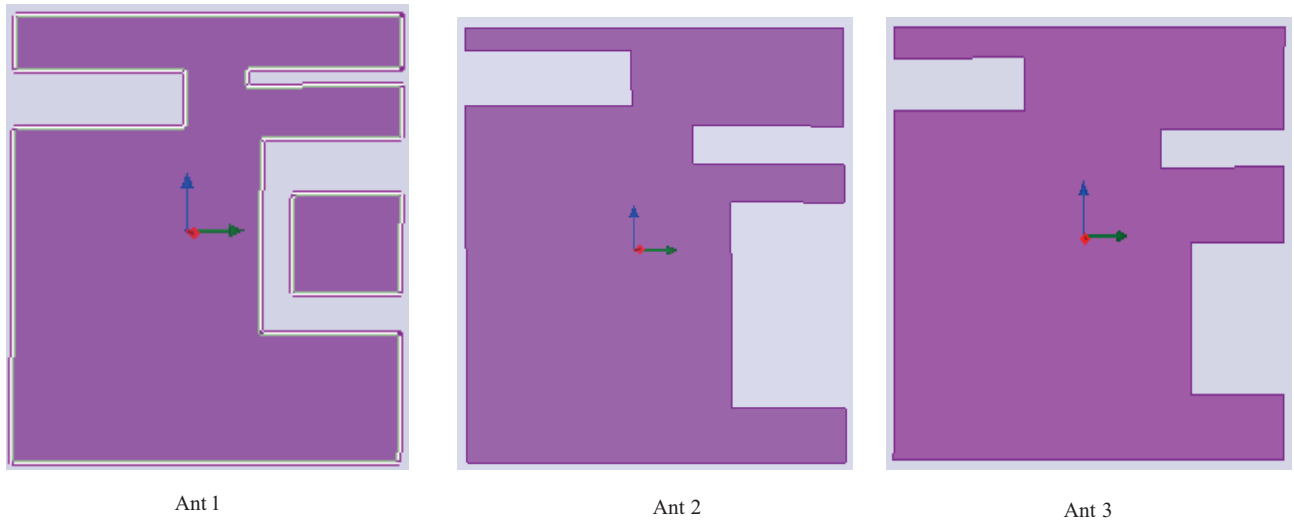


Figure 2. Improved prototypes of the single patch antenna.

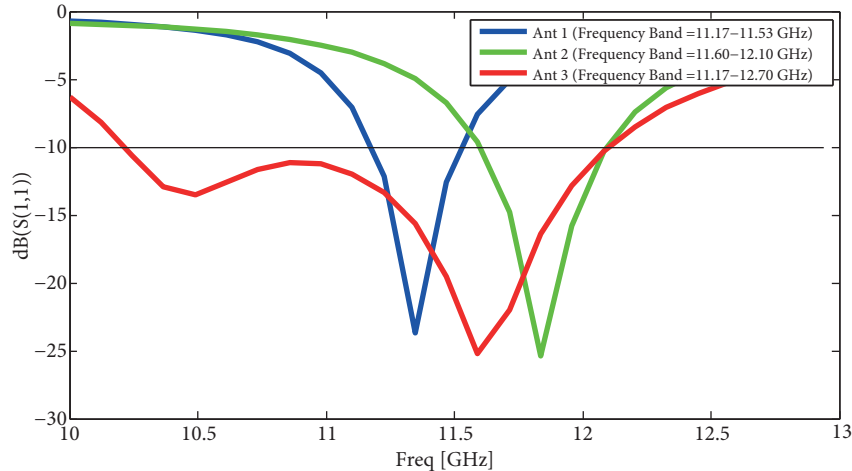


Figure 3. Improved S11 of the single patch antenna.

The proposed single patch antenna with $6.3 \text{ mm} \times 5.7 \text{ mm}$ dimensions is shown in Figure 4, with the names of parameters for different slots. Tables 1 and 2 describe the appropriate size values of the slotted patch antenna shown in Figure 4 and the simulated performance of the single patch antenna, respectively.

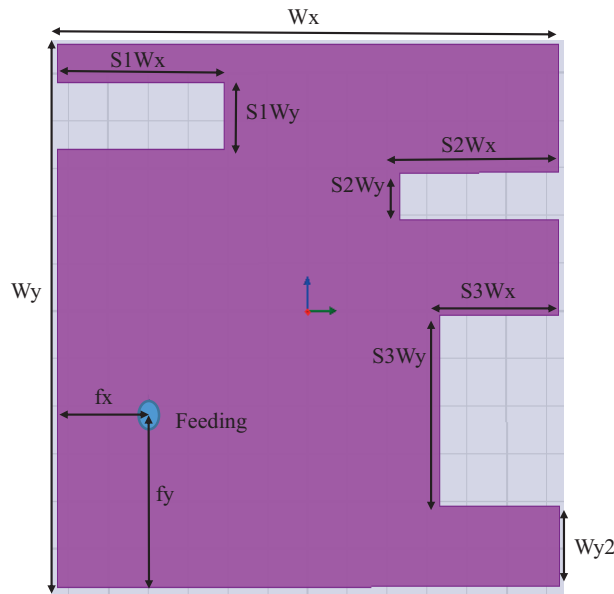


Figure 4. Novel shape of slotted patch antenna for Ku-band systems.

Table 1. Dimensions of the single antenna.

Symbol	Value (mm)	Symbol	Value (mm)
W_x	6.3	$S2W_x$	2
W_y	5.7	$S2W_y$	0.5
W_{y1}	1.35	$S3W_x$	1.5
W_{y2}	0.85	$S3W_y$	2
$S1W_x$	2.1	f_x	1.15
$S1W_y$	0.7	f_y	1.85

Table 2. Simulation performance of the single antenna.

Parameter	Value
Gain	6.6–7.0 dBi
Frequency	11.17–12.7 GHz
S_{11}	< -10 dB

Since total antenna size should be as small as possible in order to allow more solar panels, HFSS array optimization is used for finding the number of array elements and antenna positions. Therefore, from the different simulation outcomes obtained, designing 4 elements in a 2×2 array structure, which provides the desired gain and directivity, is determined. The optimized array structure and the feeding configuration of the circuit are shown in Figure 5. It can be observed from Figure 5 that the dimensions of the antenna are 16 mm (dx) \times 18 mm (dy) and the antennas are combined with a well-known 100 Ω T-junction structure ($fw1 = 1.6$ mm, $fw2 = 0.6$ mm). The feeds of each antenna element have constant amplitude and the same phase [6,7] and Taconic-TSM substrate is used ($h = 0.76$ mm) for the combiner circuit.

The performance of the array antenna is summarized in Table 3. Figure 6 displays the simulation and measurement results of the array antenna at the XZ and YZ planes. According to Figure 6, there is some backward radiation caused by the combiner circuit and because the antenna and LNA will be separated in the satellite, backward radiation is not significant for the system.

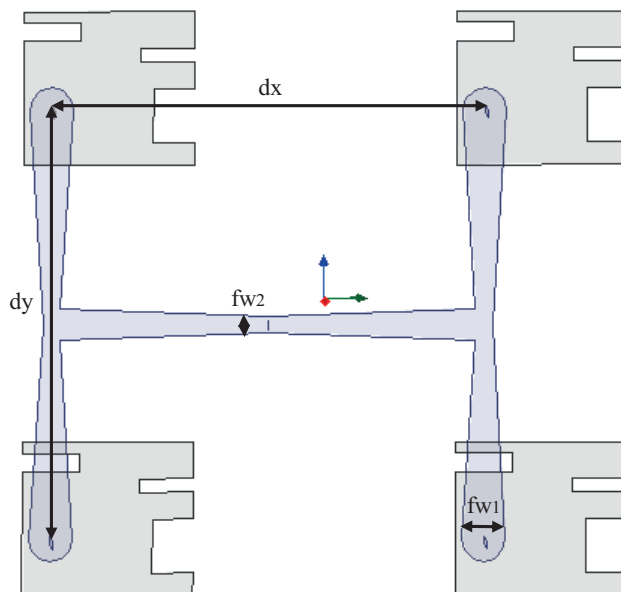


Figure 5. Top perspective view of 2×2 array antenna (combiner structure is at the very bottom).

Table 3. Measurement values of the array antenna (11.912.9 GHz).

Parameter	Value
Peak gain	10.9 dBi
-3 dB Beam width	$\pm 25^\circ$
S_{11}	< -9 dB

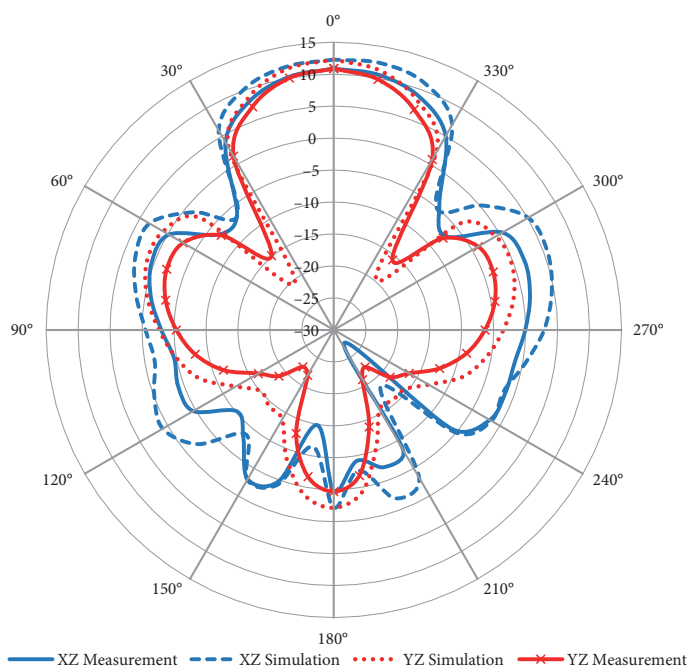


Figure 6. Radiation pattern of 2×2 array antenna at 12.5 GHz.

The proposed array antenna is fabricated with a milling-based prototype machine, and a photograph of the fabricated antenna is shown in Figure 7. The measured and simulated S parameters of the fabricated array antenna are presented in Figure 8. Measured minimum and maximum gains of the array antenna are 10.1 dBi (@12.15 GHz) and 10.9 dBi (@12.85 GHz), respectively. The printed circuit boards of the array antenna and combiner circuit (feed structure) are held together under high pressure. The center frequency of the combined system has been shifted and the integration procedure of two substrates is affected by locations and thickness of the substrates in the z direction. Differences between measurement and simulation occur because of inadequacy via the model in the simulation tool and physical changes during the mechanical processes; that is why there is also 1.4 dB gain difference between simulation and measurement.

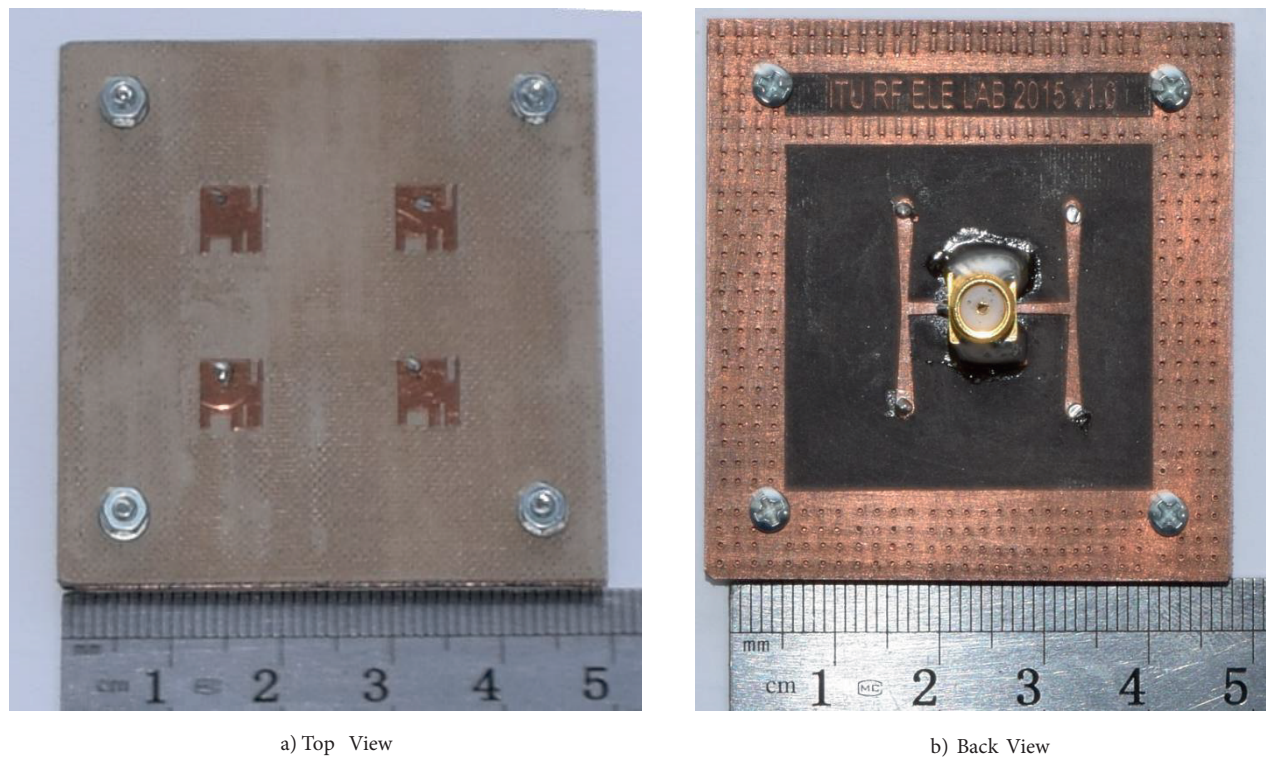


Figure 7. Top and bottom views of the fabricated antenna.

3. Low noise amplifier (LNA)

An LNA consists of three important stages: input matching stage, which is dominant for the NF; active stage, which influences gain; and the output matching stage, which affects linearity and gain [8–10] of the LNA. In this study, a small design is aimed and in order to decrease the cable losses and total NF, the designed LNA will be located near the array antenna and thus the effect of the cable loss on the total NF can be neglected.

Gain higher than 8 dB and NF lower than 1.5 dB are chosen for designing the LNA. An NEC NE3511S02 hetero junction field effect transistor (HJ-FET) is chosen for the Ku-band LNA design based on our previous studies. It has a good performance at the Ku band ($NF_{\min} = 0.3$ dB, available gain = 13.5 dB @12 GHz) and its small package (2.6 mm × 2.6 mm) is also suitable for a small PCB.

National Instruments AWR Microwave Office is used for the design and layout of the LNA. Since a nonlinear model for the selected transistor is not available for NI AWR software, S parameters are used for

the design. By considering stability carefully and doing some analysis in AWR Microwave Office, 2 V (10 mA) biasing is chosen for obtaining the desired gain and NF.

RO3003 (thickness = 0.76 mm, $\epsilon_r = 3$) is used as the substrate for designing the LNA. Figure 9 displays the circuit structure with microstrip lines and passive components. All capacitors are low ESR RF capacitors and suitable for very high frequency applications. In this work, C1 and C3 are DC blocking capacitors (1 pF) and C2 (0.2 pF) is used to increase stability. R2, R1, and R3 are 2 k Ω , 10 Ω , and 470 Ω , respectively. Additional resistors and capacitances are added to the bias line to increase stability. Rogers RF shorted $\lambda/4$ lines are used for biasing. Radial stubs are used after $\lambda/4$ lines to obtain a short circuit at the center frequency of the LNA. Figure 10 represents the layout of the designed and fabricated LNA verified by the EM tool of the NI AWR and has total dimensions of 33 mm \times 20 mm. Table 4 shows the lengths and widths of microstrip lines and the values of radial stubs.

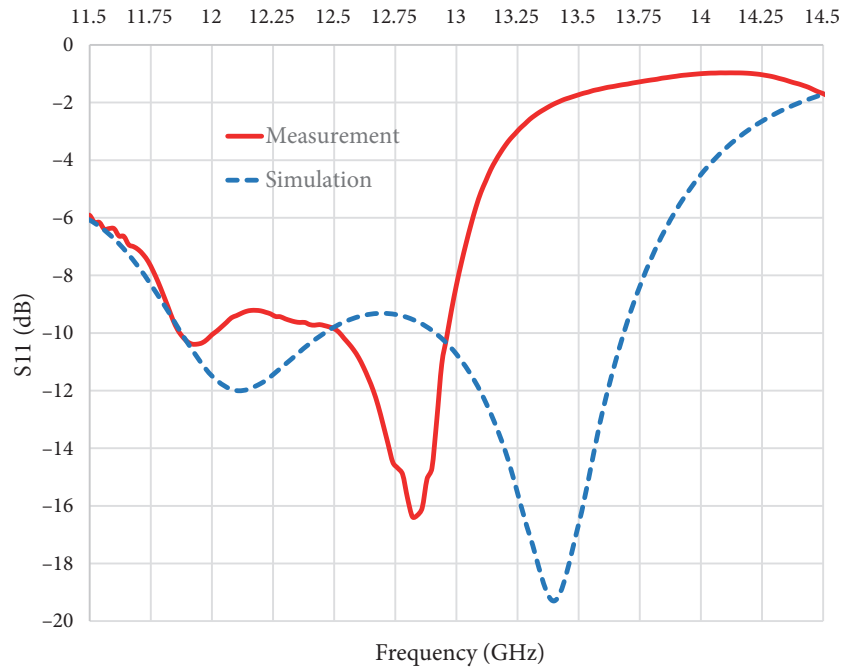


Figure 8. S_{11} simulation and measurement results of the antenna array.

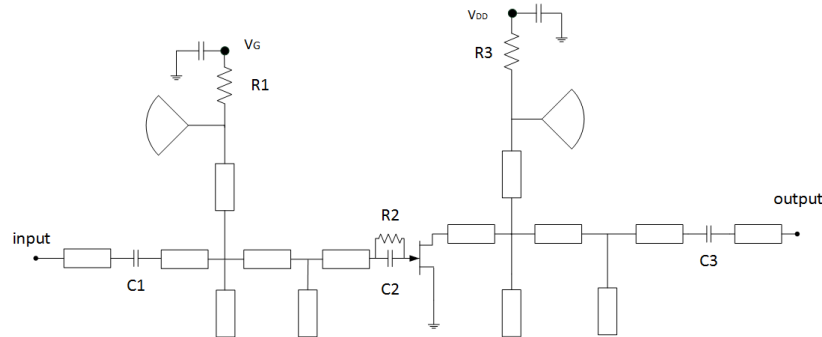


Figure 9. Structure of designed LNA.

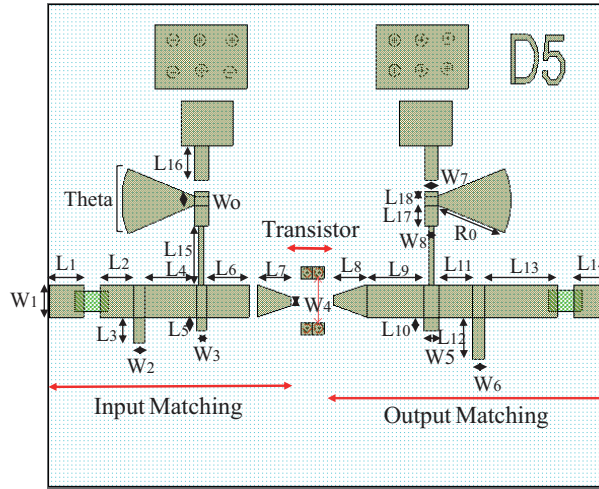


Figure 10. Layout of LNA indicating the dimensions.

Table 4. Dimensions of the transmission lines.

Length	Value (mm)	Length	Value (mm)	Width	Value (mm)
L1	2.0	L11	2.0	W0	0.55
L2	2.0	L12	2.5	W1	1.93
L3	1.5	L13	4.3	W2	0.65
L4	3.1	L14	2.0	W3	0.65
L5	0.8	L15	3.5	W4	0.54
L6	2.5	L16	2.0	W5	0.80
L7	2.0	L17	1.2	W6	0.72
L8	2.0	L18	0.3	W7	0.80
L9	3.4	R0	5.0	W8	0.30
L10	0.8	Theta	45°		

Figure 11 shows the manufactured printed circuit board of the LNA using a high accuracy milling machine that made the array antenna too. Figure 12 shows gain, NF, and reflection losses of the designed LNA and measurement values are given in Table 5. Table 6 presents some reported LNAs designed with discrete components [11,12].

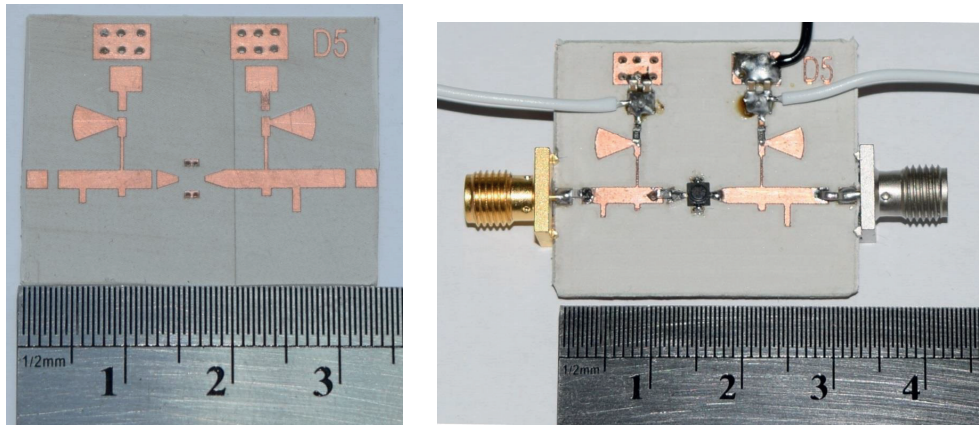


Figure 11. Fabricated LNA.

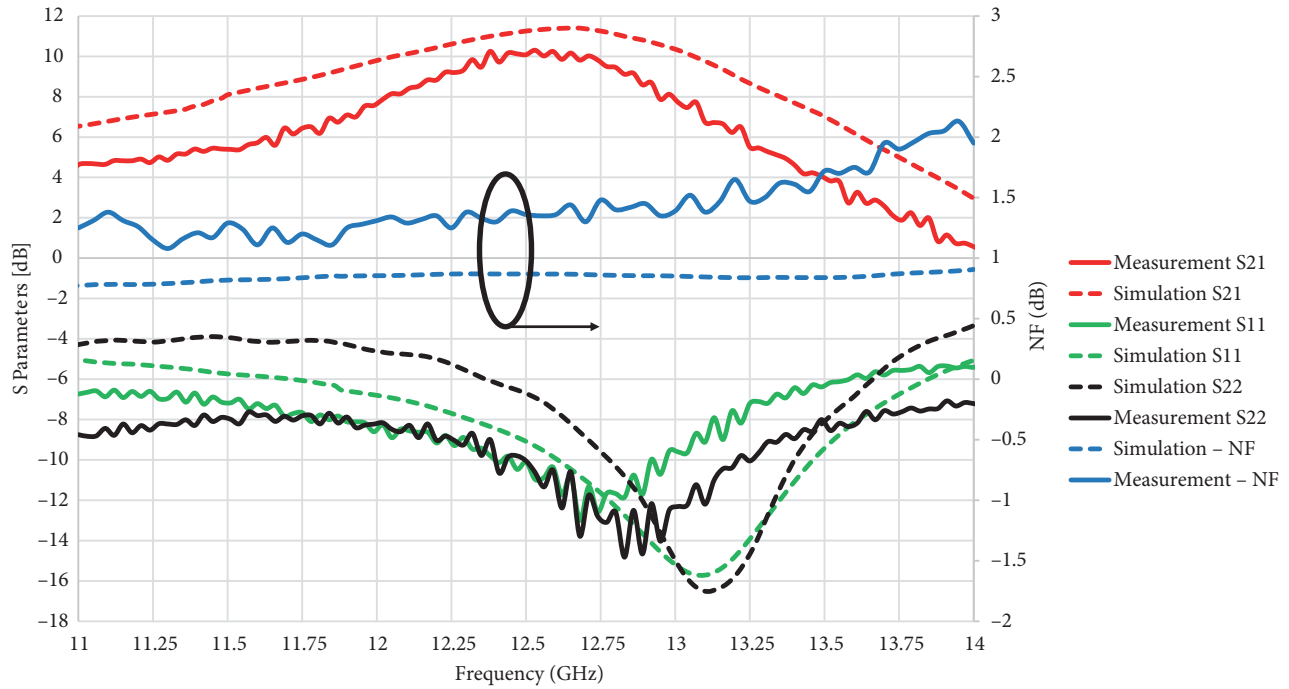


Figure 12. S parameters of simulated and fabricated LNA.

Table 5. Measurement results of LNA (12.413.0 GHz).

Parameter	Specifications
S11	< -10 dB
S22	< -10 dB
Gain	8-10.3 dB
Noise	0.9-1.45 dB

Table 6. Comparison of reported low power and discrete designs.

Ref.	Number of stages	fo [GHz]	Vds/Ids [V]/[mA]	Gain [dB]	NF [dB]
[11]	2	16	1.5/10	10.5	1.82
[12]	2	8.3	2/10	22.20	1.42
This work	1	12.6	2/10	10.1	0.9

4. Conclusion

In this study, implementations of a novel planar array antenna and LNA are presented for Ku-band small satellite receivers and they have been fabricated using a high accuracy milling machine in the laboratory. Discrete components are preferred to decrease the required time for the design and space condition verification process.

Measured minimum and maximum gains of the array antenna are 10.1 dBi and 10.9 dBi, respectively. For the LNA, in the low reflection loss band ($S_{11} < -10$ dB), the noise figure is lower than 1.5 dB (min 0.9 dB) and the gain is higher than 8 dB (max 10.3 dB) (@ 2 V, 10 mA).

During the mechanical process of the antenna assembly, some physical deformations such as via location shifting and substrate thickness change occur. Therefore, some gain difference and frequency shift appear. Measured performances of the array antenna and LNA satisfy the minimum requirements for 300 MHz bandwidth

of the transceiver system, which is planned to be used in the satellite. No additional tuning process is necessary for the implemented antenna or LNA.

Acknowledgment

This work was supported by the university scientific projects office “Bilimsel Araştırma Projeleri Koordinasyon Birimi” of İstanbul Technical University (ITU-BAP).

References

- [1] Watanabe H, Ceylan O, Saito H, Tomiki A, Nunomura H, Shigeta O, Iwakire N, Shinke T, Fukami T. High-efficiency X band GaN power amplifier for small satellite downlink system. In: IEEE MTT-S International Microwave Symposium; 2–7 June 2013; Seattle, WA, USA. New York, NY, USA: IEEE. pp. 1-4.
- [2] Misran N, Islam MT, Yusob NM, Mobashsher AT. Design of a compact dual band microstrip antenna for Ku-band application. In: ICEEI 2009 International Conference on Electrical Engineering and Informatics; 5–7 August 2003; Selangor, Malaysia. New York, NY, USA: IEEE. pp. 699-702.
- [3] Wu Q, Shi L, Zhao G. Design of a Ku-band broadband U-slot microstrip antenna. In: ICMTCE 2013 IEEE International Conference on Microwave Technology & Computational Electromagnetics; 25–28 August 2013; Qingdao, China. New York, NY, USA: IEEE. pp. 212-215.
- [4] Balanis CA. Antenna Theory: Analysis And Design. 2nd ed. Hoboken, NJ, USA: Wiley, 1997.
- [5] Prasad PC, Chattoraj N. Design of compact Ku band microstrip antenna for satellite communication. In: ICCSP 2013 International Conference on Communications and Signal Processing; 3–5 April 2013; Melmaruvathur, India. New York, NY, USA: IEEE. pp. 196-200.
- [6] Dubey SK, Pathak SK, Modh KK. High gain multiple resonance Ku-band microstrip patch antenna. In: AEMC 2011 Applied Electromagnetics Conference; 18–22 December 2011; Kolkata, India. New York, NY, USA: IEEE. pp. 1-3.
- [7] Oweis MAH, Ghouz HHM. A novel Ku-band microstrip antenna. In: ICET 2014 International Conference on Engineering and Technology; 19–20 April 2014; Cairo, Egypt. New York, NY, USA: IEEE. pp. 1-4.
- [8] Rodriguez S, Correa A, Fajardo A, Paez CI. Design and implementation of a LNA in UHF band using microstrip. In: LASCAS 2011 IEEE Second Latin American Symposium on Circuits and Systems; 23–25 February 2011; Bogota, Colombia. New York, NY, USA: IEEE. pp. 1-4.
- [9] Pozar DM. Microwave Engineering. 4th ed. Hoboken, NJ, USA: Wiley, 2012.
- [10] Othman AR, Ibrahim AB, Husain MN, Ahmad MT, Senon M. High gain, low noise Cascode LNA using T-matching network for wireless applications. In: APACE 2012 IEEE Asia-Pacific Conference on Applied Electromagnetics; 11–13 December 2012; Melaka, Malaysia. New York, NY, USA: IEEE. pp. 383-387.
- [11] Abbas T, Bin IM. Design of a two stage Low Noise Amplifier at Ku Band. In: ICM 2005 The 17th International Conference on Microelectronics; 13–15 December 2005; Islamabad, Pakistan. New York, NY, USA: IEEE. pp. 40-45.
- [12] Yılmaz M. A two stage X-band low noise amplifier optimized for minimum noise application. MSc, Bilkent University, Ankara, Turkey, 2015.